



University  
of Glasgow

Yogeswaran, N., Gupta, S. and Dahiya, R. (2018) Low Voltage Graphene FET Based Pressure Sensor. In: 2018 IEEE Sensors, New Delhi, India, 28-31 Oct 2018, ISBN 9781538647073 (doi:[10.1109/ICSENS.2018.8589569](https://doi.org/10.1109/ICSENS.2018.8589569)).

This is the author's final accepted version.

There may be differences between this version and the published version. You are advised to consult the publisher's version if you wish to cite from it.

<http://eprints.gla.ac.uk/186086/>

Deposited on: 21 May 2019

Enlighten – Research publications by members of the University of Glasgow  
<http://eprints.gla.ac.uk>

# Low Voltage Graphene FET Based Pressure Sensor

Nivasan Yogeswaran, Shoubhik Gupta, Ravinder Dahiya\*

<sup>1</sup>Bendable Electronics and Sensing Technologies (BEST) Group, University of Glasgow, G12 8QQ, UK

\*Correspondence to: [Ravinder.Dahiya@glasgow.ac.uk](mailto:Ravinder.Dahiya@glasgow.ac.uk)

**Abstract**— This paper presents a low voltage graphene field effect transistor (GFET) based pressure sensor. The sensor comprises of GFET connected with a piezoelectric Aluminium Nitride (AlN) capacitor in an extended gate configuration. In this configuration, the piezopotential generated across the AlN capacitor, as a result of applied pressure, appears at the gate terminal of GFET and modulates the channel current. The sensor operates at a remarkably low voltage (100mV) and exhibits a sensitivity of about  $7.18 \times 10^{-3} \text{ Pa}^{-1}$  for a pressure range of 3.25-9.74 kPa. These values make the developed GFET sensor suitable for tactile skin in robotics and prosthetics and for wearable health monitoring devices.

**Keywords**— Aluminum Nitride, Extended Gate, GFET, Tactile sensor, Solid-State Sensor.

## I. INTRODUCTION

Pressure sensors are vital components of tactile skin in robotics and prosthetics [1, 2] They are also increasing in demand for other applications such as touch screens for portable electronics [3], wearable health monitoring [4, 5] and electronic skin (e-skin) [6] etc. As a result, a number of novel device architectures and transduction mechanisms have been explored for pressure or touch sensing. These include capacitive [7, 8], piezoresistive [9, 10], piezoelectric [11] and optical [12] mechanisms etc. Many of the applications require these sensors to be highly sensitive, fast and to have low power operation. In this regard, pressure sensors with organic transistors, GFET and conventional silicon based field effect transistor (FET) have been explored in various configurations such as active matrix [13-15], and extended gate [16, 17] etc. These sensors have elastomeric dielectric [7], air (dielectric) [14] and piezoelectric layers [11] etc. connected to or deposited on the transistors. In particular, the piezoelectric capacitors based on lead zirconate titanate (PZT)[18] [19], polyvinylidene fluoride-trifluoroethylene (P(VDF-TrFE)) [11, 20] have been used with transistors.

A major issue with the piezoelectric materials, particularly as transducer on top of a transistors or in extended gate configuration, is related to the requirement of high voltage ( $\sim 100\text{V}/\mu\text{m}$ ) to orient the dipoles and hence to introduce piezoelectric properties [11] [19]. Application of such a high voltage near to the transistor could damage the devices or permanently alter their electrical characteristics. In such a situation, a piezoelectric material which does not require poling would be ideal. Another issues with several of the FET based pressure sensors, particularly those based on organic transistors, is that they require high operation voltage ( $\sim 60\text{V}$ ) which also lead to high-power consumption and limits their use in large area e-skin and other portable device applications [21]. Recently, low-voltage operation in organic transistors has been demonstrated, however the large area implementation is yet to come [17, 20].

This work was supported by Engineering and Physical Science Research Council (EPSRC) Fellowship for Growth – Printable Tactile Skin (EP/M002527/1).

Addressing the issues of poling and low-voltage operation, this paper presents Graphene FET (GFET) based pressure sensors. The sensor comprises of GFET tightly coupled with AlN piezo-capacitor. Owing to its well oriented crystal structure, AlN does not require poling. The high chemical and thermal stability of AlN and ability to deposit piezoelectric AlN film via low temperature process such as sputtering [22] also make it an attractive material for the development of touch sensors on flexible substrates. The use of GFET, instead of conventional transistors, is explored here for low-voltage low-power operation. Indeed, with GFET, the sensor operates at a remarkably low voltage of 100mV. Graphene's high carrier mobility and intrinsic mechanical properties lend high sensitivity to the sensors. With recent results showing the transfer of graphene on large area flexible substrates [8, 23] it will be possible to extend the presented approach to obtain fast touch sensors on flexible substrates.

The paper is organised as follows: Section II presents the working and fabrication of presented sensor. The device characterisations are presented in Section III. Finally, a summary of key outcomes is given in Section IV.

## II. WORKING PRINCIPLE AND FABRICATION

The pressure sensor consists of 2 main components: (a) GFET (b) Metal-Insulator-Metal (MIM) AlN capacitor. The AlN MIM structure is capacitively coupled to top gate of GFET as shown in Fig. 1.

### A. Working Principle of Sensor.

AlN is a piezoelectric material which generates a voltage on application of mechanical stress. The AlN MIM structure connected in an extended gate configuration acts as the transduction layer of presented pressure sensor. The application of a mechanical stress results in the generation of a piezopotential across AlN capacitor. In the extended gate configuration (Fig. 1), this piezopotential also appears at the gate of GFET and results in the modulation of channel current.

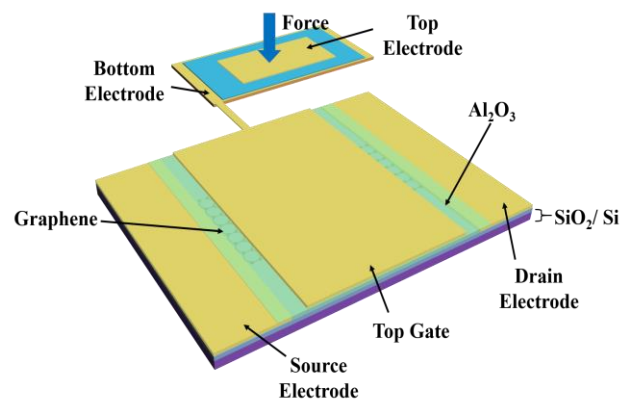


Fig. 1. Scheme of the pressure sensor with AlN capacitor connected to GFET in an extended gate configuration.

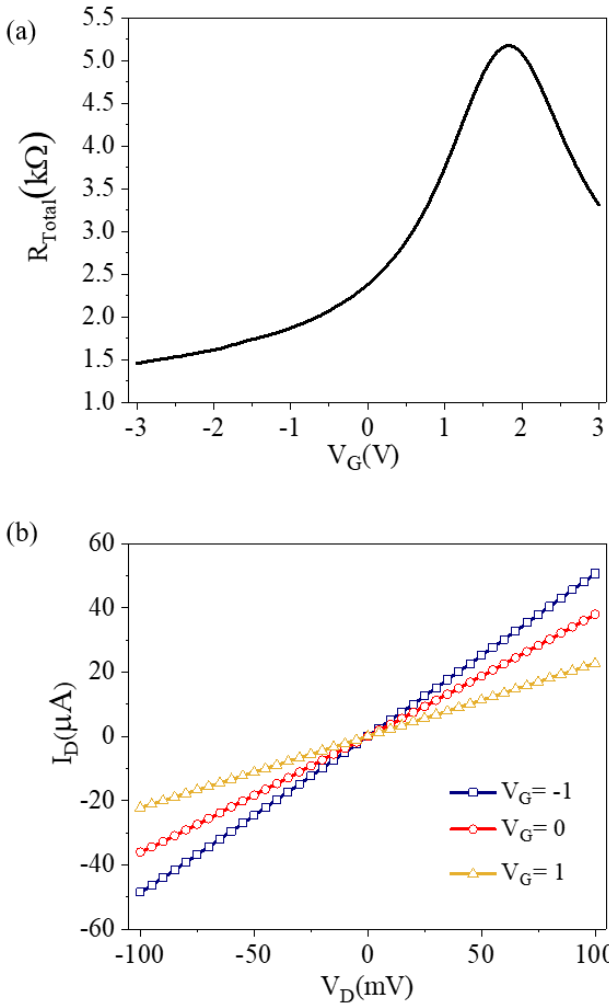


Fig.2. Electrical characterisation of GFET (a) Total resistance of GFET at  $V_{ds}=100\text{mV}$  (b) Output characteristics of GFET.

Therefore, change in the channel current reflects the applied pressure.

### B. Fabrication of GFET

The fabrication of the top-gate GFET was initiated by wet transfer of graphene to  $\text{SiO}_2/\text{Si}$  substrate using cellulose acetate butyrate (CAB) as supporting layer. The elaborate details of the transfer process is explained elsewhere [24]. Following the transfer printing of graphene, the source and drain electrodes (10 nm/50 nm Ti/Au) were defined by photolithography, metallization and lift-off. The metallization of the electrodes was carried out using Plassys MEB 550S E-Beam evaporator. The definition and isolation of graphene channel was carried out by using a photolithography and reactive ion etching (RIE) in  $\text{O}_2$  plasma at 300W for 13s using Oxford Instruments RIE 80+ resulting in  $50\mu\text{m}$  channel width. A 2nm Al was deposited in  $\text{O}_2$  ambient prior to the atomic layer deposition (ALD) of top gate dielectric  $\text{Al}_2\text{O}_3$ . A 30nm of  $\text{Al}_2\text{O}_3$  was deposited at  $200^\circ\text{C}$  via thermal ALD process with trimethylaluminium (TMA) and  $\text{H}_2\text{O}$  as the precursors using Oxford Instruments FlexAL Atomic Layer Deposition. Following the ALD growth of  $\text{Al}_2\text{O}_3$ , top gate electrode (10nm /60 nm Ti/Au) was deposited via photolithography, metallization and lift-off resulting in a top gate length of  $45\mu\text{m}$ . Finally, vias to the source and drain electrodes were opened via etching using  $\text{HF}:\text{H}_2\text{O}$  (1:100) with photoresist acting as the etch mask.

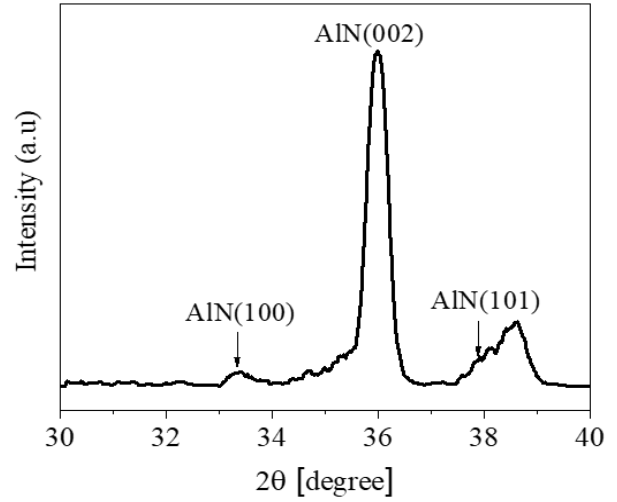


Fig.3. XRD of RF sputtered AlN film showing a strong c-axis peak associated with piezoelectric property of AlN.

### C. AlN MIM fabrication.

The piezoelectric AlN MIM structure was fabricated on a flexible polyimide substrate. The deposition of AlN was carried out in a low temperature RF sputtering process. A 500nm thick AlN was sputtered on top of 100nm Al deposited on polyimide substrate. AlN was deposited via RF magnetron sputtering with Al as target using Plassys MP 900s sputtering system. The sputtering was carried out in  $\text{N}_2$  and Ar atmosphere with flow rate of 40 sccm and 20sccm respectively under a 3mTorr pressure and 700W RF power. Prior to sputtering, pre-sputtering was carried out for 5 min with a closed shutter. Following the deposition of AlN film the MIM structure was completed by deposition of top electrode (NiCr/Au-20 nm /100 nm). The deposition of top electrode was carried out using a hard mask and electron beam evaporation.

## III. DEVICE CHARACTERIZATION

### A. GFET Characterisation

The electrical characterization of GFET was performed at room temperature using the Keysight B1500A semiconductor device parameter analyzer. The results from electrical characterization of GFET are shown in Fig. 2. The carrier mobility of the GFET was extracted using the fitting model proposed by Kim et al [25]. The hole and electron mobility of the GFET was extracted via separate fitting owing to the asymmetry of hole and electron branch around the Dirac point. The hole and electron mobility of the device are  $868$  and  $718 \text{ cm}^2/\text{V.s}$  respectively.

### B. AlN Characterisation

The crystal structure of the sputtered AlN film was studied using X-ray diffraction (XRD) Panalytical Xpert Pro MRD. The XRD scan was performed between the range of  $30^\circ$ - $40^\circ$ . The XRD results of the sputtered film is shown in Fig.3. The sputtered film exhibited a strong peak related (002) plane at  $2\theta = 36.03^\circ$  while the peak associated (100) and (101) can also be observed at  $2\theta = 33.3^\circ$  and  $37.9^\circ$  respectively. In addition, the peak observed at  $2\theta=38.4^\circ$  is associated with the reflection from the bottom Al electrode of the MIM structure.

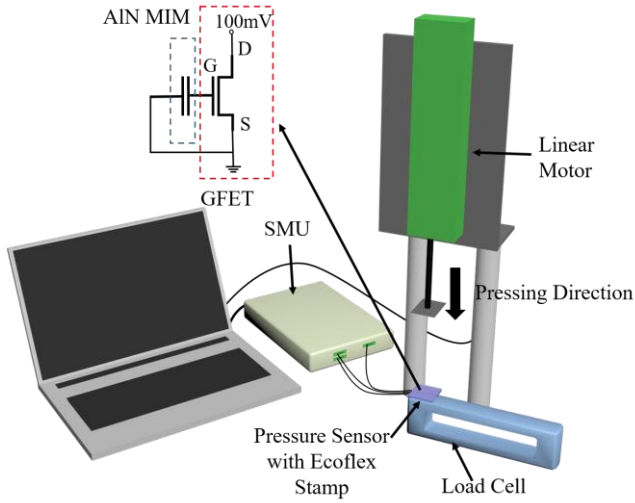


Fig.4. Illustration of the experimental setup for pressure sensor characterisation. The biasing condition of the sensor during the sensor characterisation is also shown.

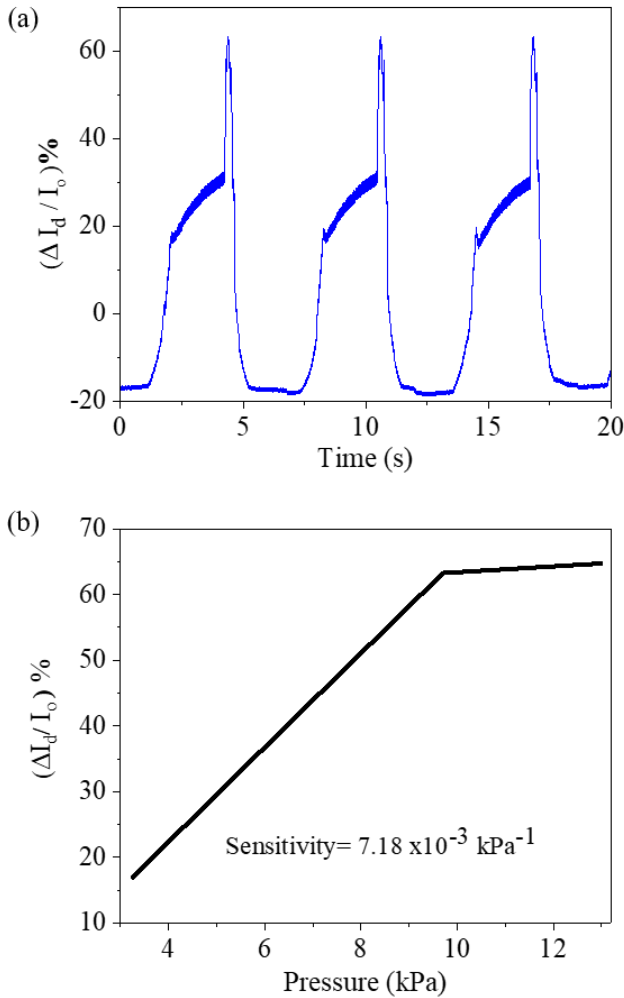


Fig.5. (a) Dynamic response of the sensor to pressure 9.74 kPa (b) Sensitivity of the sensor for varying magnitude of pressure in the range of 3.25-9.74 kPa.

### C. Pressure Sensor Characterization and operation mechanism

The performance of the sensor was evaluated by varying applied pressure ranging from 0 kPa- 13 kPa. The response of the sensor to varying magnitude of force was studied using an in-house pressure sensing setup. The schematic of the experimental setup used for the characterization of the sensor is shown in Fig. 4. The setup comprises of a linear motor (VT-21 Linear stage from MICRONIX USA) and load cell. The movement of the motor was controlled by LabVIEW program. Prior to the application of force, the magnitude of applied force was calibrated using a load cell. During the pressure sensing characterization, the sensor was biased using a Keysight USB Modular source modular unit (SMU-U2722A) The sensors was covered with a 150 $\mu$ m thick Ecoflex which served as a protective layer during the application of force. The dynamic response of the sensor to applied pressure of 3.25kPa is shown in Fig 5a. During sensor characterization, the transistor was biased at the following condition:  $V_{ds} = 100\text{mV}$ ; and top gate voltage of GFET at 0V with the extended gate connected to the top gate of GFET as shown in Fig 4. The application of force to AIN MIM generates a piezopotential, which also appears at the gate of GFET and modulates the channel current. The sensor response to different applied pressures is shown in Fig 5b. The device exhibits a sensitivity of  $7.18 \times 10^{-3} \text{ Pa}^{-1}$  for a pressure range between 3.25-9.74 kPa with a limit of detection of 0.89 kPa. Sensitivity of the device is given by  $(\Delta I/I_o) / \Delta P$ , where  $\Delta I$  is the change in the drain current and  $I_o$  is the initial drain current and P is the applied pressure. The sensor demonstrates an excellent sensitivity within the low pressure regime (1-10 kPa) which is ideal for applications related to intra body pressure measurements and object manipulations [26].

### IV. CONCLUSIONS

In summary, this reported low voltage pressure sensor is reported here with GFET in an extended gate configuration connected to a piezoelectric AIN MIM capacitor. The use of AIN as a piezoelectric transduction layer evades the need of poling which otherwise a detrimental effect on the transistors due to application of high electric field used during the process. Notably, the sensor operates at a very low voltage of 100mV which is attractive for wearable electronics and e-skin applications. In addition, the sensor has been developed by adopting a low temperature CMOS compatible process which would enable the use of sensors for large area flexible electronics applications. The developed sensor exhibited an excellent sensitivity in low pressure regime (1-10 kPa) which is attractive for the for application related to wearable health monitoring and e-skin applications [26]. The performance and sensor's spatial resolution could be further improved by integrating the piezoelectric layer within the dielectric stack of the film.

### ACKNOWLEDGEMENT

The authors are thankful to the support received for this work from James Watt Nanofabrication Centre (JWNC) and Electronic Systems Design Centre (ESDC).

## REFERENCES

- [1] R. S. Dahiya, G. Metta, M. Valle, and G. Sandini, "Tactile Sensing-From Humans to Humanoids," *IEEE Trans. Robot.*, vol. 26, pp. 1-20, 2010.
- [2] R. S. Dahiya and M. Valle, *Robotic Tactile Sensing: Technologies and System*: Springer Science & Business Media, 2013.
- [3] S. Gao, X. Wu, H. Ma, J. Robertson, and A. Nathan, "Ultrathin Multifunctional Graphene-PVDF Layers for Multidimensional Touch Interactivity for Flexible Displays," *ACS Appl. Mater. Interfac.*, vol. 9, pp. 18410-18416, 2017.
- [4] T. Sekitani, U. Zschieschang, H. Klauk, and T. Someya, "Flexible organic transistors and circuits with extreme bending stability," *Nat. Mater.*, vol. 9, p. 1015, 2010.
- [5] A. Paul, M. A. Kafi, and R. Dahiya, "Paper based pressure sensor for green electronics," in *IEEE SENSORS*, Glasgow, 2017, pp. 1-3.
- [6] N. Yogeswaran, W. Dang, W. T. Navaraj, D. Shakthivel, S. Khan, E. O. Polat, *et al.*, "New materials and advances in making electronic skin for interactive robots," *Advanced Robotics*, vol. 29, pp. 1359-1373, 2015.
- [7] G. Schwartz, B. C. K. Tee, J. Mei, A. L. Appleton, D. H. Kim, H. Wang, *et al.*, "Flexible polymer transistors with high pressure sensitivity for application in electronic skin and health monitoring," *Nat. Commun.*, vol. 4, p. 1859, 2013.
- [8] C. N. García, W. T. Navaraj, E. O. Polat, and R. Dahiya, "Energy - Autonomous, Flexible, and Transparent Tactile Skin," *Adv. Funct. Mater.*, vol. 27, p. 1606287, 2017.
- [9] N. Yogeswaran, S. Tinku, S. Khan, L. Lorenzelli, V. Vinciguerra, and R. Dahiya, "Stretchable resistive pressure sensor based on CNT-PDMS nanocomposites," in *2015 11th Conference on Ph.D. Research in Microelectronics and Electronics (PRIME)*, Glasgow, 2015, pp. 326-329.
- [10] S. Qijun, K. D. Hwan, P. S. Sik, L. N. Yoon, Z. Yu, L. J. Heon, *et al.*, "Transparent, Low - Power Pressure Sensor Matrix Based on Coplanar - Gate Graphene Transistors," *Adv. Mater.*, vol. 26, pp. 4735-4740, 2014.
- [11] R. S. Dahiya, G. Metta, M. Valle, A. Adami, and L. Lorenzelli, "Piezoelectric oxide semiconductor field effect transistor touch sensing devices," *Appl. Phys. Lett.*, vol. 95, p. 034105, 2009.
- [12] M. Ramuz, C. K. T. Benjamin, B. H. T. Jeffrey, and Z. Bao, "Transparent, Optical, Pressure - Sensitive Artificial Skin for Large - Area Stretchable Electronics," *Adv. Mater.*, vol. 24, pp. 3223-3227, 2012.
- [13] R. S. Dahiya, A. Adami, C. Collini, and L. Lorenzelli, "POSFET tactile sensing arrays using CMOS technology," *Sens. Actuator A-Phys.*, vol. 202, pp. 226-232, 2013.
- [14] S.-H. Shin, S. Ji, S. Choi, K.-H. Pyo, B. Wan An, J. Park, *et al.*, "Integrated arrays of air-dielectric graphene transistors as transparent active-matrix pressure sensors for wide pressure ranges," *Nat. Commun.*, vol. 8, p. 14950, 2017.
- [15] T. Someya, T. Sekitani, S. Iba, Y. Kato, H. Kawaguchi, and T. Sakurai, "A large-area, flexible pressure sensor matrix with organic field-effect transistors for artificial skin applications," *Proc. Natl. Acad. Sci. USA*, vol. 101, pp. 9966-9970, 2004.
- [16] I. Graz, M. Kaltenbrunner, C. Keplinger, R. Schwödiauer, S. Bauer, S. P. Lacour, *et al.*, "Flexible ferroelectret field-effect transistor for large-area sensor skins and microphones," *Appl. Phys. Lett.*, vol. 89, p. 073501, 2006.
- [17] F. A. Viola, A. Spanu, P. C. Ricci, A. Bonfiglio, and P. Cosseddu, "Ultrathin, flexible and multimodal tactile sensors based on organic field-effect transistors," *Sci. Rep.*, vol. 8, p. 8073, 2018.
- [18] N. Yogeswaran, W. T. Navaraj, S. Gupta, F. Liu, L. Lorenzelli, V. Vinciguerra, *et al.*, "Piezoelectric Graphene Field Effect Transistor Pressure Sensors for Tactile Sensing," *Appl. Phys. Lett.*, 2018 (in press).
- [19] C. Dagdeviren, Y. Su, P. Joe, R. Yona, Y. Liu, Y.-S. Kim, *et al.*, "Conformable amplified lead zirconate titanate sensors with enhanced piezoelectric response for cutaneous pressure monitoring," *Nat. Commun.*, vol. 5, p. 4496, 2014.
- [20] S. Hannah, A. Davidson, I. Glesk, D. Uttamchandani, R. Dahiya, and H. Gleskova, "Multifunctional sensor based on organic field-effect transistor and ferroelectric poly(vinylidene fluoride trifluoroethylene)," *Org. Electron.*, vol. 56, pp. 170-177, 2018.
- [21] Y. Zang, F. Zhang, D. Huang, X. Gao, C.-a. Di, and D. Zhu, "Flexible suspended gate organic thin-film transistors for ultra-sensitive pressure detection," *Nat. Commun.*, vol. 6, p. 6269, 2015.
- [22] M. Schneider, A. Bittner, and U. Schmid, "Impact of film thickness on the temperature-activated leakage current behavior of sputtered aluminum nitride thin films," *Sens. Actuator A-Phys.*, vol. 224, pp. 177-184, 2015.
- [23] E. O. Polat, O. Balci, N. Kakenov, H. B. Uzlu, C. Kocabas, and R. Dahiya, "Synthesis of Large Area Graphene for High Performance in Flexible Optoelectronic Devices," *Sci. Rep.*, vol. 5, p. 16744, 2015.
- [24] N. Yogeswaran, D. Shakthivel, L. Lorenzelli, V. Vinciguerra, and R. Dahiya, "Graphene gold nanoparticle hybrid based near infrared photodetector," in *2017 IEEE SENSORS*, Glasgow, 2017, pp. 1-3.
- [25] S. Kim, J. Nah, I. Jo, D. Shahrjerdi, L. Colombo, Z. Yao, *et al.*, "Realization of a high mobility dual-gated graphene field-effect transistor with Al<sub>2</sub>O<sub>3</sub> dielectric," *Appl. Phys. Lett.*, vol. 94, p. 062107, 2009.
- [26] Y. Zang, F. Zhang, C.-a. Di, and D. Zhu, "Advances of flexible pressure sensors toward artificial intelligence and health care applications," *Mater. Horizons*, vol. 2, pp. 140-156, 2015.